

WAVELET ANALYSIS OF THE SOLAR ROTATIONAL ACTIVITY VARIATIONS

*R.Werner (1), A.Hempelmann (2), D.Valev (1), I. Kostadinov (1,3),
At.Atanassov (1), G.Giovanelli (3), A.Petritoli (3), D.Bortoli (3),
F.Ravegnani (3)*

*(1) Solar-Terrestrial Influences Laboratory, Stara Zagora Department,
BAS, Bulgaria*

(2) Hamburg Observatory, Hamburg University, Hamburg, Germany

(3) Institute of Atmospheric Science and Climate, Bologna, CNR, Italy

Introduction

The study of the solar activity has been of great interest for a long time. On the one hand it is important for the understanding of the Sun as an active star and on the other hand – for the investigations of the solar-terrestrial connections.

The solar magnetic field reverses approximately every 22 years, and manifests the 11-year solar cycle, in which the Sun changes its activity from its maximum to its minimum value. The activity variations, developed by the sun surface rotation in connection with the nonsymmetrical distribution of active regions over the solar disc are in a shorter time scale. As it is well known, these variations have periods of about 27 days. The amplitude of the solar irradiance variations is strongly dependent on its wavelength and increases towards shorter wavelengths. Over a solar cycle, the total solar irradiance changes with only 0.1%, yet in the UV and shorter wavelengths they exceed those by orders of magnitude [1]. The changes in this spectral range are of basic importance for the solar-terrestrial influences and require detailed analysis of the growth and decay of active regions, because the EUV solar irradiance is fully absorbed by the Earth atmosphere, and the UV irradiation is absorbed partially.

27-day Solar Cycle

In the sense of the statistical average, in the beginning of the solar cycle, the active regions originate at heliographic mid latitudes Φ and shift equatorwards with the cycle extension. The solar surface rotates with different velocity, depending on the latitude. The differential solar rotation period, observed from the Earth, can be approximated with sufficient

accuracy by: $P_{\text{syn}} = 26.75 + 5.7 \sin 2\Phi$ [2]. A wider spread of the solar activity indices is observed, however, around the 27-days period. At first, the 27 periodicity is non-sinusoidal and higher harmonics can appear in the spectra. Donnelly and Puga have shown that the second harmonic (the 13.5 day oscillation) is of physical nature and includes predominantly two groups of activity regions with a phase shift of approximately 180° [3]. A 12-14 day period is obvious in most indices, related to chromospheric emissions, such as the CaII-K plage index, but is absent in the F10.7. Generally, however, the periodicities range from 20 to 36 days. It is pointed out that the indices with “periodicities around 30-34 days shifted to about 26-28 days in 1982“, when the Sun was in a maximum activity phase. Bouwer concludes that the “period is a result of the combination of active-region evolution and solar rotation (i.e. not due to the differential rotation)“[4] A reason for the widely spread periodicities around 27 days is that the dominant radiance within an active region can move rapidly forward or backward in respect to the solar surface [5]. The power spectra of projected areas of active and passive spots show the 27-day rotation, active spots besides 28 and 25, 51 and 157 day periodicities [6]. Bai remarks that the periodicity at approximately 25 and 50 days are maybe harmonics of the Rieger’s period (about 150 days) [6].

Data set preparation

For our analysis we have used the CaII-K-line index from the Big Bear Solar Observatory (BBSO) for the time period from 1996 until 2003 (<ftp://ftp:bbso.njii.edu/pub/archive/>). The index is determined by Sun images in the K-line (393.9 nm) with a 1.5\AA FWHM filter, obtained by a CCD camera. Indices are formed by integrating the brightness above thresholds of 0% (D0 index), 2.5% (D25), 5% (D50 7.5% (D75) and 10% (D100). The pixel numbers above the threshold at 7.5% produce the plage area index (D75A - index 05 in the BBSO data archive). It is expected that the correlation between the indices and the solar $L\alpha$ irradiation is the best for the D0 index, since the network is more prominent in the $L\alpha$ flux. While for higher thresholds weak networks are cut and plages and bright network spots are dominant, in the images stronger 27-day modulations are provided by higher D-indices. The year 1996 is approximately the solar activity minimum and in October the current 23rd solar cycle 23 begins (see Fig. 1). In particular, the analysis is carried out with the CaII-K line plage area D75A-index, which shows strong rotational modulation and for the comparison - the D0-index. To represent the 27-day rotational modulation,

the time series are divided into two parts. The first one includes the last part of the solar minimum before October 1996 and the increased solar activity phase up to the end of 1999 and, the second one includes the solar maximum and the start of the decline phase. In the data set the only missing

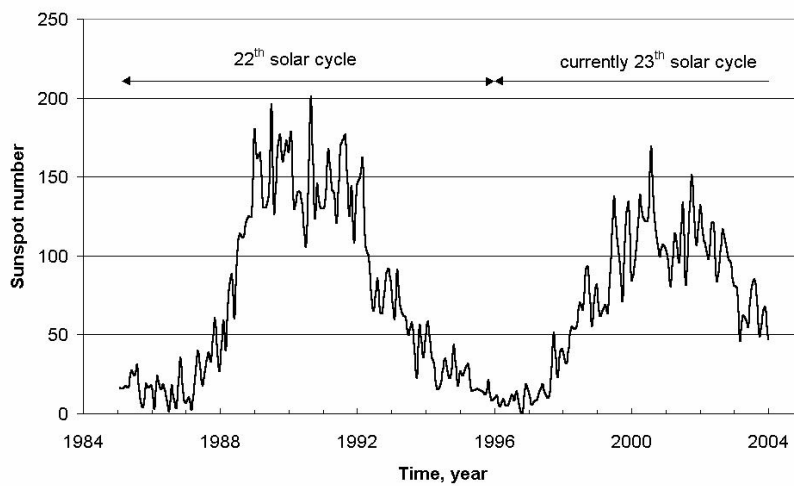


Fig 1. The 11-year solar activity evolution during the last and the currently solar cycle, expressed by the Greenwich Sun spot number. It is accepted, that in October 1996 was started the currently 23th solar cycle.

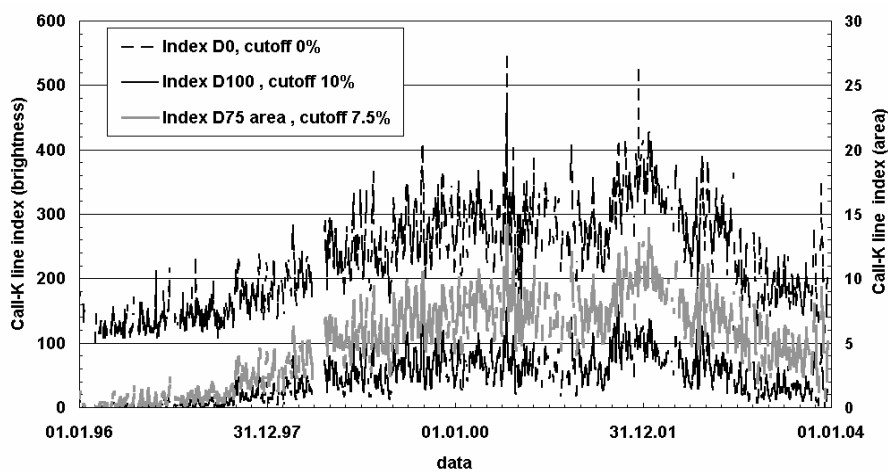


Fig. 2 Time evolution of the D00, D100 and D75A CaII-K line index from 1. January 1999 up to 31.December 2003. The indices D25, D50 and D75

values (not shown) are located between D0 and D100 from greater to smaller brightness respectively to increased thresholds.

data are for successive days over a time interval of some days and very rarely of a longer period. The missing data are linearly interpolated (with the values at the interval end points) and for intervals longer than 5 days, the corresponding day number is stored. Smoothed by running mean over 41 days series were subtracted from the interpolated time series to bring out the periods about 27 days. For data gaps longer than 5 days the values of the time difference series are set to zero, because the interpolated values over larger time intervals differ strongly from the real values. As seen in Fig. 2 the rotational amplitudes are very different during the different activity phases. They are very small at the solar minimum and then they continuously increase with the activity increase. For the time period 1996-1999 the obtained 27-rotation variation of the index has been divided by solar activity, approximated by a low order polynomial. The changes of the activity indices by the Sun rotation are much more regular around the solar maximum and additional data processing is not necessary.

Simple solar activity model

The CaII K line time series shows, that the short-time periods are modulated by periods of several months (see also Fig 4 and 5). The obtained behaviour can be described in first approximation by a simple model, which consists of a harmonic oscillation with simultaneous amplitude and phase modulation:

$$B = A \cos[(t - t_1) \omega],$$

where A is the amplitude modulation:

$$A = 1 + \cos[(t - t_2) \omega_1],$$

and ω is the phase modulation:

$$\omega = \omega_0 \{1 + d * \cos[(t - t_3) \omega_2]\},$$

and t_1, t_2, t_3 are the phase shifts. The Period of the Sun rotation is T_0 and it is chosen to 27-days and ω_0 is the corresponding angular frequency. The period of the amplitude modulation ω_1 is selected to several Sun rotations. We have fixed ω_1 to $n\omega_0$, with $n=8$. (n is not required to be an integer number). We have set the phase shifts t_1 to $T_0/2$ and t_2 to $nT_0/2$. In that way the amplitude maximum of A is reached at the half of the period length. We have studied only the influence of the phase shift t_3 . The modulation index d is fixed at 0.1. For a further simplification $\omega_1 = \omega_2$ is set. Thus, the phase

modulation describes the growth or decay of the period during the active region evolution expressed by amplitude modulation A. (For results see Fig. 3)

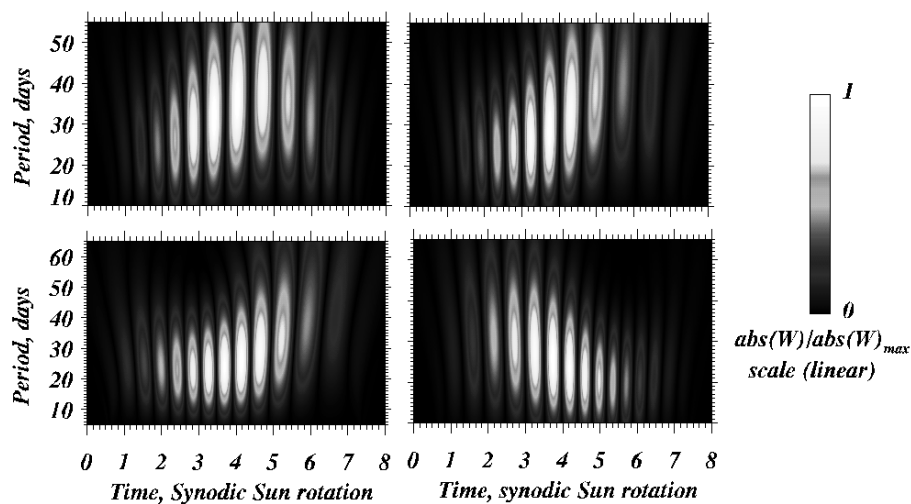


Fig. 3 Wavelet spectra of the modeled solar activity for the time of the first amplitude period for some phase shifts t_1 . Top: left $t_1=T_0$, the maximum of the amplitude of solar rotation activity variation is in coincidence with the maximum of the amplitude modulation located at 4 Sun rotations, right $t_1=3T_0$, the period of solar activity slowly increased, however the maximum of its amplitude is reached before the period maximum and the activity decrease suddenly, bottom, $t_1=5T_0$ the maximum of the solar activity variation is in coincidence with the minimum of reached period, and right $t_1=7T_0$. The solar activity at the beginning of signal is relatively low but the period is high, with increasing of the time the period is decreasing and after the transition of the activity maximum it is decay. It is obiose high frequency corresponding to a 20 day period.

Wavelet basics

A new tool – the wavelet analysis, is successfully applied in the last years for analysis of geophysical time series [8,9]. Hempelmann has developed a method to determine the duration of the Sun differential rotation [10] and for stars, rotating as slow as the Sun [11]. Soon and Baliunas have found by wavelet time frequency approach that the rotation of some chromospheric active stars is at least 10 years long [12]. The long-

period solar activity wavelet analysis was carried out by Le [13]. A wavelet is a function and satisfies the conditions of:

zero mean
$$\int_{-\infty}^{\infty} \psi(t) dt = 0$$

(i)

and additionally the normalization
$$\|\psi\| = 1 .$$

(ii)

(It should be noted that the condition (ii) under certain circumstances is equivalent to the criteria of the regularity). The continuous wavelet transformation (WT) W_{ψ} for a given mother wavelet of a time signal $f(t)$, is defined as:

$$W_{\psi} f(a, b) = \int_{-\infty}^{\infty} f(t) \psi_{a,b}^*(t) dt$$

with the complex conjugate wavelet function

$$\psi_{a,b} = \frac{1}{a^{1/2}} \psi\left(\frac{t-b}{a}\right),$$

where $\psi_{a,b}$ represents the mother wavelet ψ , shifted by b and dilated/compressed by a . The factor $1/a^{1/2}$ satisfies the normalization condition. Since the beginning of the eighties, when the wavelet theory was first developed, many mother wavelets have been found. The simplest of them are the Haar- and Morlet-wavelets and the Mexican hat. In the following

$$\psi = \left[1 - (ct)^2\right] e^{-(ct)^2/2}, \quad \text{with } c =$$

4

is used as a mother wavelet [14]. This is the so-called Mexican hat wavelet, because the graph of this function is similar to them. The Mexican hat is a simple real function and the calculation of WT is comparatively fast. Moreover, the function is symmetric, which is useful for identifying regions of maximum/minimum curvature [15]. In analogy to FT, the spectrum is given by $|W_{\psi} f|$ and the power spectrum by $|W_{\psi} f|^2$. The result of the WT $W_{\psi}(a,b)$ is defined in the phase plane, spanned by the time shift b and the scaling parameter a . For the chosen wavelet with $c = 4$ the scale parameter a at maximum and minimum of $W_{\psi}(a,b)$ presents directly the

signal period. For the interpretation of the wavelet spectrum it is important to note that the frequency resolution for constant b is proportional to $1/a$ and it decreases with the increase of ω , but the time resolution increases with the decrease of a . This is the typical wavelet zoom effect. In consideration of the frequency filtering of a given time series it should be noted that WT is similar to a convolution (For $a = 1$ the WT is exactly the convolution of the time signal $f(t)$ with the analyzed wavelet.) The time series are filtered by a more stretched /compressed filter function (mother wavelet) by increasing/decreasing scale parameter a . The resulting wavelet spectra are given at the fig. 4 and 5.

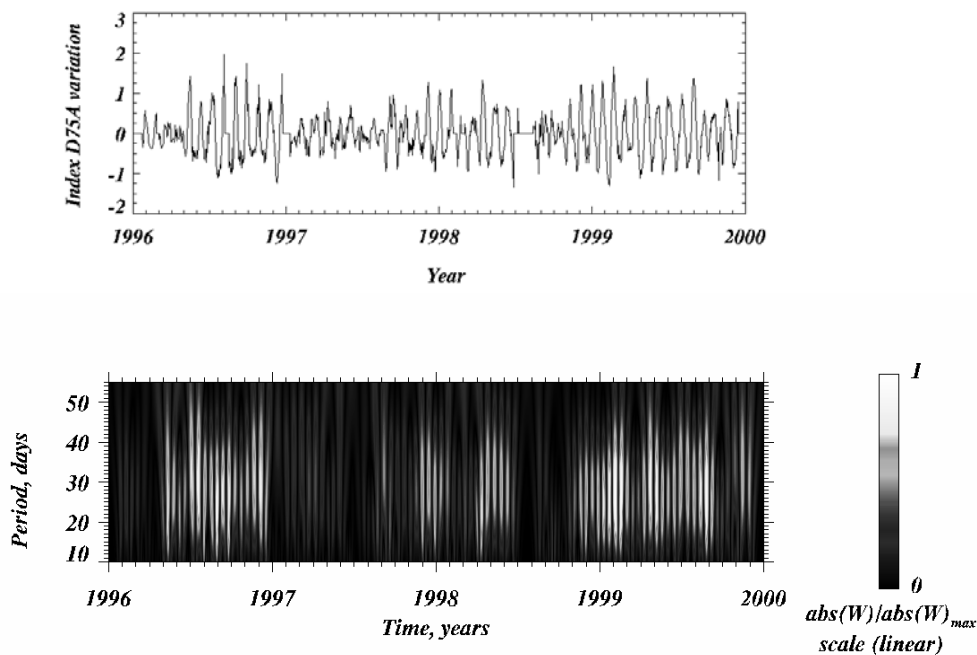


Fig 4. a) Long time removed time series of the CaII-K line core index for the minimum between the 22 and the 23rd solar cycle 1.Jan. 1996 up to increase par of the 23rd cycle 31.Dec.1999. (For processing details see the text) b) The wavelet spectrum of the time series shown at a)

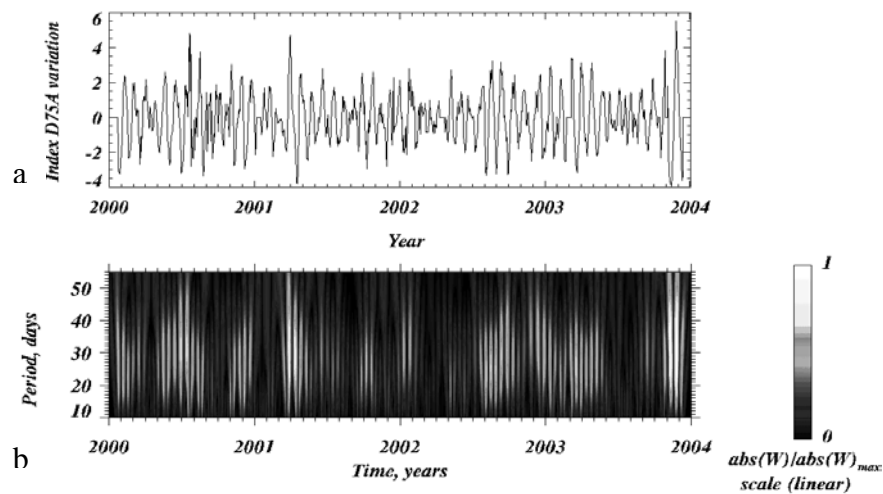


Fig 5. a) Long time removed time series of the CaII-K line core index for the maximum of the 23rd solar cycle 1.Jan. 2000 and the begin of the decreasing phase pu to 31.Dec.2003 b) The wavelet spectrum of the time series shown at a

Results

The time series have displayed obvious packets with period lengths of several months, modulating the solar activity variation caused by the rotation cycle. This period is probably related to active region growth and decay, i.e. the typical lifetime of a single spot group or an active region. The areas and the brightness of an active region decay/grow after the plage formation. The parent spot of a bipolar group of a developing region travels slightly forward with increasing the distance to the subsequent spot. With decrease of the active region, the parent spot shifts backward nearly to its initial heliographic longitude, the bright remnants always trailing behind and towards the poles. The appearance or the decay of new regions changes the activity distribution over the solar disc. These processes modify the observed rotation period. The wavelet analysis of the shows clearly a change of the period from 22 up to 34 days, which is significantly longer than that, predicted only by the differential sun rotation.

Conclusions

The simple solar activity model, which takes into account phase and amplitude modulations, can be used to explain that the periods due to the solar 27-rotation cycle are in a range of 22 up to 34 days and both kinds of modulation are consequence of activity region growth or decay, hence, they are a result of a variable pattern of spots and active regions on the solar surface. The areas and the brightness of an active region grow after the plage formation. The parent spot of a bipolar group of a developing region travels slightly forward with increasing the distance to the following spot. With decrease of the active region, the parent spot shifts backward nearly to its initial heliographic longitude, the bright remnants always trailing behind and towards the poles. The appearance or the decay of new regions changes the activity distribution over the solar disc. These processes modify the observed rotation period. The wavelet analysis shows clearly a change of the period from 22 up to 34 days, which is significantly longer than that, predicted only by the differential sun rotation. We have described the variability of the longer period by amplitude modulation, while the shortening and the prolongation of the solar rotation period can be modeled by a phase modulation. The superimposing modulations change the period more than twice by nonlinear effects. The proposed simple empirical model describes with good quality the separate episodes of the active region evolution. Both kinds of modulation are the consequence of activity region growth or decay and hence, they are a result of a variable pattern of spots and active regions on the solar surface.

The applied method based on wavelet analysis is very useful to study of the duration of several solar periods and its progress.

References

1. Fligge, M, S.K. Solanki, The solar spectral irradiance since 1700, *Geophys. Res. Lett.* Vol. 27, No. 14, 2157 – 2160
2. Lang, K.R. *Astrophysical Data: Planet and Stars*, Springer-Verlag New York etc., 1992, 104
3. Donnelly, R.F. and L.C.Puga, *Solar Physics*, vol. 130, 1990, 369
4. Bower, S.D. , Periodics of solar irradiance and solar activity indices, II, *Solar Physics*, 142 (1992) pp. 365 - 389
5. Kane, R.P, Fluctuations in the ~ 27-daz sequences in the solar index F10 During solar cycles 22-23, *Journ. Atmos. Solar-Terr. Phys.*,65, 2003, 1169 – 1174
6. Pap, J., W.K.Tobiska, S.D.Bower, Periodics of solar irradiance and solar activity indices, I, *Solar Physics*, 129, 1990, 165 - 189
7. Bai, T, Periodicities in Solar Flare Occurrence: Analysis of Cycles 19-23, *The Astrophysical Journal*, vol.591, Issue 1, 406-415.

8. Liu, H.-S. and B.F.Chao Wavelet Spectral Analysis of the Earth's Orbital Variations and Paleoclimatic Cycles, *Journal of Atmospheric Sciences*, vol 55, no.2, 1996, 227 – 236
9. Liu, P.C. Wavelet Spectrum Analysis and ocean Wind waves, *Wavelets in Geophysics* ed. by E.Foufoula-Georgiou and P.Kumar, Academic Press, 1994, 151 - 166
10. Hempelmann, A. and R.A. Donahue, Wavelet Analysis of Stellar Differential Rotation I. The Sun, *Astronomy and Astrophysics*, vol. 322, 1997, 835
11. Hempelmann, A., Wavelet Analysis of Stellar Differential Rotation: III. The Sun in white light, *Astronomy and Astrophysics*, vol. 399, 2003, 717-721
12. Soon, W. and Baliunas, S., Lifetime of Surface features and Stellar Rotation: A Wavelet Time-Frequency Approach, *the Astrophysics Journal*, vol. 510, iss.2, 1999, L135 –L 138
13. Le, G.-M., Wavelet Analysis of Several Important Periodic properties in the Relative Sunspot Numbers, *Chinese Journal of Astronomie and Astrophysics*, vol. 3, No.5, 2003, 391 -394
14. Weinberg, B.L., S.R.Drayson and K.Freese, Wavelet Analysis and Visualisation of the Formation and evolution of two total ozone events over northern Sweden, *Geophys. Res. Let.*, vol. 23, No. 17, August 15, 1996, 2223 - 2226
15. Hageberg, C.R. and N.K.K.Gamage, Application of Structure preserving Wavelet Decompositions to Intermittent Turbulence: A Case Study, *Wavelets in Geophysics* ed. by E.Foufoula-Georgiou and P.Kumar, Academic Press, 1994, 45-80